



# EPA Public Access

Author manuscript

*Nanotoxicology*. Author manuscript; available in PMC 2020 August 01.

About author manuscripts

Submit a manuscript

Published in final edited form as:

*Nanotoxicology*. 2019 August ; 13(6): 795–811. doi:10.1080/17435390.2019.1578428.

## ***In vitro* intestinal toxicity of copper oxide nanoparticles in rat and human cell models**

**Taylor E. Henson<sup>1</sup>, Jana Navratilova<sup>2</sup>, Alan H. Tennant<sup>3</sup>, Karen D. Bradham<sup>4</sup>, Kim R. Rogers<sup>4</sup>, Michael F. Hughes<sup>3</sup>**

<sup>1</sup>Student Services Contractor, Research Triangle Park, NC 27711

<sup>2</sup>National Research Council, Research Triangle Park, NC 27711

<sup>3</sup>National Health and Environmental Effects Research Laboratory, Office of Research and Development, U.S. Environmental Protection Agency, Research Triangle Park, NC 27711

<sup>4</sup>National Exposure Research Laboratory, Office of Research and Development, U.S. Environmental Protection Agency, Research Triangle Park, NC 27711

### **Abstract**

Human oral exposure to copper oxide nanoparticles (NPs) may occur following ingestion, hand-to-mouth activity, or mucociliary transport following inhalation. This study assessed the cytotoxicity of CuO and Cu<sub>2</sub>O-polyvinylpyrrolidone (PVP) coated NPs and copper ions in rat (IEC-6) and human intestinal cells, two- and three-dimensional models, respectively. The effect of pre-treatment of CuO NPs with simulated gastrointestinal (GI) fluids on IEC-6 cell cytotoxicity was also investigated. Both dose- and time-dependent decreases in viability of rat and human cells with CuO and Cu<sub>2</sub>O-PVP NPs and Cu<sup>2+</sup> ions was observed. In the rat cells, CuO NPs had greater cytotoxicity. The rat cells were also more sensitive to CuO NPs than the human cells.

Concentrations of H<sub>2</sub>O<sub>2</sub> and glutathione increased and decreased, respectively, in IEC-6 cells after a 4-h exposure to CuO NPs, suggesting formation of reactive oxygen species (ROS). These ROS may have damaged the mitochondrial membrane of the IEC-6 cells causing a depolarization, as a dose-related loss of a fluorescent mitochondrial marker was observed following a 4-h exposure to CuO NPs. Dissolution studies showed that Cu<sub>2</sub>O-PVP NPs formed soluble Cu whereas CuO NPs essentially remained intact. For GI fluid-treated CuO NPs, there was a slight increase in cytotoxicity at low doses relative to non-treated NPs. In summary, copper oxide NPs were cytotoxic to rat and human intestinal cells in a dose- and time-dependent manner. The data suggests Cu<sub>2</sub>O-PVP NPs are toxic due to their dissolution to Cu ions, whereas CuO NPs have inherent cytotoxicity, without dissolving to form Cu ions.

---

Send correspondence to: Michael Hughes, U.S. Environmental Protection Agency, MD B105-03, Research Triangle Park, NC, USA 27711, hughes.michaelf@epa.gov, Fax: 919-541-4284.

Disclosure of interest

The authors report no conflict of interest.

**Publisher's Disclaimer:** Disclaimer: The research described in this article has been reviewed by the U.S. EPA and approved for publication. Approval does not signify that the contents necessarily reflect the views or the policies of the Agency. Mention of trade names or commercial products does not constitute endorsement or recommendation for use.

## Keywords

intestine; nanoparticles; copper oxide; *in vitro*; toxicity; reactive oxygen species

---

## Introduction

Metallic nanoparticles (NPs), such as the metal oxides, are used in industrial processes (e.g., catalyst), in commercial products (e.g., sunscreen) and as anti-microbial agents (Chang et al., 2012; McSweeney 2016; Vimbela et al., 2017). One class of metal oxide NPs are the copper oxides, which are found in oxidation states of I and II. Copper oxide NPs are used in a range of applications due to their high surface reactivity, chemical stability during catalytic reactions, thermoelectric properties and superconductivity. Due in part to this surface reactivity, copper oxide NPs have toxicological properties. Cupric (II) oxide (CuO) NPs are cytotoxic to several human cell lines including A549 (human alveolar) (Karlsson et al., 2008; Wang et al., 2012a), TT-1 (transformed human alveolar type 1) (Misra et al., 2014), Caco-2 cells (Ude et al., 2017) and HEp-2 (larynx epithelium) (Fahmy and Cormier, 2009). *In vitro* effects of CuO NPs include cytostasis and genotoxicity in murine macrophages (Di Bucchianico et al., 2013) and release of pro-inflammatory cytokines by TT-1 cells (Misra et al., 2014). Cuprous (I) oxide (Cu<sub>2</sub>O) NPs induce apoptosis in HeLa and melanoma cells at concentrations lower than in normal human and mouse cell lines (Wang et al., 2012b). A stress-induced mechanism involving the endoplasmic reticulum by Cu<sub>2</sub>O NPs appears to have a role in apoptosis of renal carcinoma cells (Yang et al., 2017). Formation of reactive oxygen species (ROS), reduction of cellular glutathione, and mitochondrial membrane depolarization have been observed in cells exposed to CuO NPs (Thit et al., 2015; Wang et al., 2012a). Cu<sub>2</sub>O NPs also produce ROS and damage mitochondrial membranes (Wang et al., 2012b). One proposed mechanism of toxicity of metal oxide NPs is the release of toxic ions (Fröhlich, 2013); toxicity of CuO and Cu<sub>2</sub>O NPs may be due to release of Cu ions. However, some studies suggest that the CuO NPs have inherent toxicological properties; that is, toxicity of CuO NPs is not totally from dissolution and release of Cu ions (Karlsson et al., 2008; Midlander et al., 2009).

Exposure to NPs may occur by inhalation, ingestion and dermal contact (reviewed in Kermanizadeh et al., 2015; Landsiedel et al., 2012). Once inhaled into the lungs, NPs may be absorbed into the systemic circulation or transported from the lungs to the pharynx via the mucociliary lining the pulmonary tract and swallowed. While dermal contact with NPs can occur, their systemic absorption through the skin appears to be limited. Some NPs may enter hair follicles or the stratum corneum, but further penetration to the viable epidermis is extremely curtailed (Elder et al., 2009; Landsiedel et al., 2012). Ingestion of NPs may occur incidentally by hand-to-mouth activity, from the diet of contaminated food or water, or swallowing material inhaled and transported to the pharynx. Information on the effect of NPs on the gastrointestinal (GI) tract following ingestion is lacking. NPs may be absorbed systemically by this route, but the mechanism of absorption is not well defined. NPs may injure the epithelial lining of the GI tract, which may increase their systemic absorption. The stability and agglomeration of ingested NPs may also be affected by GI fluids (Lefebvre et al., 2015).

The objective of this study was to assess the cytotoxicity of two copper oxide NPs in a two-dimensional rat intestinal model and a three-dimensional human intestinal model. Three-dimensional cellular models of human tissue offer more similarity to human tissue *in vivo* than two-dimensional cellular models (Antoni et al., 2015). The three-dimensional intestinal model used in this study has cellular polarity, villi and brush border membranes. The NPs tested varied in valence and surface modification. As a source of Cu<sup>1+</sup> and Cu<sup>2+</sup> ions, CuCl and CuSO<sub>4</sub>, respectively, were also tested. In addition, CuO NPs treated with simulated GI fluids were tested for cytotoxicity. A potential mechanism of toxicity, generation of ROS, was also investigated.

## Materials and Methods

### Chemicals

Cupric (II) oxide (CuO) nanopowder (diameter < 50 nm by transmission electron microscopy (TEM); surface area, 29 m<sup>2</sup>/g; information from manufacturer) was purchased from Sigma Aldrich (Lot. No MKBJ4678V, St. Louis, MO). NanoXact cuprous (I) oxide (Cu<sub>2</sub>O) nanoparticle colloids (diameter, 48 ± 7 nm by TEM; hydrodynamic diameter, 266 nm; surface area, 20 m<sup>2</sup>/g; information from manufacturer) in water (1 mg/mL) and coated with polyvinyl pyrrolidone (PVP) were purchased from nanoComposix (Lot No. HXJ01358, San Diego, CA). PVP used as a NP capping agent can minimize particle aggregation. Triton X-100, cuprous sulfate pentahydrate and t-butyl hydrogen peroxide were purchased from Sigma Aldrich. Cupric chloride was from Fisher Scientific (Hampton, NH).

### Transmission Emission Microscopy

The size and morphology of nanoparticles were evaluated by transmission electron microscopy (TEM). Samples were prepared by depositing a drop of the nanoparticle suspension (100 µg/mL Dulbecco's Modified Eagle Medium with 10% fetal bovine serum) onto a carbon-coated nickel grid and allowing it to dry in air overnight at room temperature. Micrograph images were obtained using an FEI Titan 80–300 probe aberration corrected scanning TEM with a monochromator operating at 200 kV. A Bruker 4 SDD Energy Dispersive Spectroscopy (EDS) instrument was used to perform elemental mapping. Images were acquired at 300 kV. The TEM image for the Cu<sub>2</sub>O-PVP nanoparticle suspension was provided by nanoComposix ([www.nanocomposix.com](http://www.nanocomposix.com)).

### Rat and human intestinal models

Rat small intestine epithelial cells (IEC-6) were purchased from American Type Culture Collection (ATCC®, Manassas, VA). This non-transformed cell line is a two-dimensional model of the rat small intestine. The adherent cells were grown using Dulbecco's Modified Eagle Medium (DMEM) (ATCC®) with 4 mM L-glutamine, 1.5 g/L sodium bicarbonate, 4.5 g/L glucose, 10% by volume fetal bovine serum (FBS) (ATCC®) and 1% by volume penicillin/streptomycin solution (100×, Corning Life Sciences, Tewksbury, MA). A 0.25% solution of Gibco Trypsin-EDTA (Thermo Fisher Scientific, Waltham, MA) was used to detach cells from culture plates. IEC-6 cells were seeded in clear 96-well (60,000 cells/well) coated plates, complete media added and placed overnight in an incubator set at 37 °C, 95% relative humidity and 5% CO<sub>2</sub>. The following day the cells were treated with test material.

Following addition of test material to the wells, the plates were returned to the incubator for either 4 or 24 h.

A three-dimensional model of the human small intestine, EpiIntestinal™ (SMI-100), was purchased from MatTek Corp. (Ashland, MA). This model is a highly differentiated epithelium consisting of villi structures, brush borders and columnar epithelium. The tissue is cultured with an air-liquid interface in 6-well plates with media below the tissue. Media (DMEM, phenol-red; gentamicin, 5 µg/mL; amphotericin B, 0.25 µg/mL; epidermal growth factor and other proprietary factors) and Triton X-100 (used as the positive control) were included with the assay kit. Following receipt, the media was changed and the tissue was equilibrated overnight in an incubator set at 37 °C, 95% relative humidity and 5% CO<sub>2</sub>. The next day the cells were treated with test material in fresh media. The plates were returned to the incubator for either 4 or 24 h.

### Treatment of intestinal models with nanoparticle preparations and ionic copper solutions

Ten mg of CuO nanopowder (8 mg Cu) was weighed into a glass vial and 10 mL of media was added. This mixture was probe sonicated ( $3 \times 4.5 \text{ W} \times 3 \text{ seconds}$ ) (Sanders et al. 2012) and aliquots at various concentrations were prepared for dosing of rat and human intestinal models. The 1 mg/mL (0.9 mg Cu/mL) solution of Cu<sub>2</sub>O-PVP NPs in water was diluted to 100 µg/mL Cu<sub>2</sub>O (89 µg Cu/mL) in media, probe sonicated and dilutions were prepared before application to the cells. Time between sonication of the NPs, dilution and delivery to the cells was minimized (i.e., minutes). Copper (II) sulfate was dissolved in media at a concentration of 1 mg/mL (0.8 mg Cu/mL) and diluted. This solution was used as a source of Cu<sup>2+</sup> ions. Copper (I) chloride was dissolved in media warmed to 37 °C at a concentration of 1 mg/mL (0.8 mg Cu/mL), vigorously vortexed and diluted. This solution was used as a source of Cu<sup>1+</sup> ions. The effect of dose of the two NPs and CuSO<sub>4</sub> on IEC-6 cell viability was assessed at concentrations of 0.1 – 100 µg/mL (0.08 – 89 µg Cu/mL, see Supplementary Table 1); in EpiIntestinal cells, the concentrations were 1 – 100 µg/mL (0.8 – 89 µg Cu/mL). CuCl was tested only in IEC-6 cells at a concentration range of 0.1 – 100 µg/mL (0.08 – 80 µg Cu/mL). Aliquots of sonicated CuO and Cu<sub>2</sub>O-PVP NPs dosing preparations were analyzed by a zetasizer (Malvern Instruments, Westborough, MA) for hydrodynamic diameter, polydispersion index and zeta potential after dosing (i.e., time 0 h) and at either 4 or 24 h after dosing.

### Cell viability measurement

IEC-6 cell viability was measured using 3-(4,5-dimethylthiazol-2-yl)-5-(3-carboxymethoxyphenyl)-2-(4-sulfophenyl)-2H-tetrazolium (MTS) (Sigma-Aldrich). After either a 4- or 24-h exposure to the nanoparticles, CuCl or CuSO<sub>4</sub>, the media was removed and the cells were washed 3 times with phosphate buffered saline (PBS) (37 °C) and replaced with 100 µL media and 20 µL MTS. The plates were returned to the incubator for 1–4 h, and then absorbance was measured at 490 nm with a SpectraMax i3 (Molecular Devices, Sunnyvale, CA) plate reader.

Viability of the human intestinal model was measured using 3-(4,5-dimethylthiazol-2-yl)-2,5-diphenyltetrazolium bromide (MTT). MTT is the recommended viability assay by

the vendor for this model. After either a 4- or 24-h exposure to the NPs or CuSO<sub>4</sub>, media was aspirated, and the cells were washed 3 times with PBS (37 °C). After the addition of 300 µL of MTT solution to each well, the plates were returned to the incubator for 3 h. Excess MTT solution was removed and 1 mL per well of isopropanol was added to extract the formed formazan (reduced product of MTT) from the cells. After a 1 h extraction, an additional 1 mL of isopropanol was added and each well was mixed thoroughly before absorbance was measured at 570 nm with the plate reader. (Note: we began our studies with the rat IEC-6 cells and chose to use the MTS assay because it does not require an extraction step of the reduced formazan. We moved onto the human EpiIntestinal model and the manufacturer recommended that the MTT assay be used to measure viability.)

Nanoparticles have been noted to interfere with some cell viability assays (Holder et al., 2012; Petersen et al., 2014). The cells were washed with PBS three times before addition of MTS or MTT, which should remove non-absorbed NPs. Incubating CuO NPs (80 µg Cu/mL) with MTS or MTT resulted in no color change of the tetrazolium compounds (i.e., reduction). CuO NPs did not inhibit the direct reduction of MTS or MTT by ascorbic acid (1 mM).

### **Microscopic analysis of IEC-6 cells**

Before viability of IEC-6 cells treated with NPs was assessed, cells were imaged using a Nikon Diaphot microscope (Nikon Instruments, Melville, NY) with phase contrast and a Leica 40× objective. Pictures were taken with a Paxcam 2 microscope camera (MIS, Inc., Villa Park, IL).

### **Dissolution of CuO and Cu<sub>2</sub>O-PVP NPs**

To evaluate the temporal stability of copper-based NPs in cell media, 30 mL of DMEM with 10% FBS was spiked with CuO NPs or PVP-coated Cu<sub>2</sub>O NPs at a total concentration of 10 µg Cu/mL and incubated at 37 °C for up to 24 h. As a positive control, CuSO<sub>4</sub> in water or media was used. A 5-mL subsample was removed at time intervals of 0, 1, 2, 4 and 24 h. Each subsample was then centrifuged through a 10 kDa filter (Amicon Ultra-15, 10 K, Millipore, Bedford, MA) at 5911g for 20 min. One mL of each filtrate was hot plate digested at 60°C with 1 mL concentrated HNO<sub>3</sub> (SCP Science, Baie D'Urfé, Quebec, Canada) overnight. The digested filtrates were diluted with deionized water to a final volume of 10 mL and directly analyzed by inductively coupled plasma optical emission spectroscopy (ICPOES) (Thermo Scientific, Waltham, MA, USA) for total copper content. The ICPOES calibration range was 0.01–2 ppm with a method detection limit of 10 ppb.

### **Simulated gastrointestinal fluid treatment of CuO NPs and IEC-6 cellular viability assessment**

The effect of simulated gastrointestinal fluids on CuO NPs and potential alteration on cytotoxicity in IEC-6 cells was assessed. The procedure as outlined by McCracken et al. (2013) was followed. Briefly, CuO NPs (1 mg/mL; 0.8 mg Cu/mL) were incubated in water (pH 2 – 6) with pepsin (from porcine gastric mucosa, 146 U/mL, Sigma Aldrich) for 1 h at 37 °C and ultracentrifuged (Beckman-Coulter, Indianapolis, IN; 60,000 rpm, 45 min, 4°C). The pellet was resuspended in water (pH 7), incubated with pancreatin (from porcine

pancreas, 2 mg/mL, Sigma Aldrich) for 1 h at 37 °C and ultracentrifuged. The pellet was suspended in water (pH 7), incubated in porcine bile extract (Sigma Aldrich) for 1 h at 37 °C and ultracentrifuged. Before each centrifugation step, an aliquot of the treated NPs was analyzed in the zetasizer for measurement of hydrodynamic diameter, polydispersity index and zeta potential. After the last centrifugation step, the particles were suspended in media, sonicated, and diluted as described above. Cytotoxicity in IEC-6 cells was assessed as described previously for 4 or 24 h using the CuO NPs treated with pepsin at pH 2, and pancreatin and bile salts at pH 7.

### Detection of H<sub>2</sub>O<sub>2</sub>

The formation of H<sub>2</sub>O<sub>2</sub> produced following addition of CuO NPs to IEC-6 cells was assessed using the ROS-Glo™ H<sub>2</sub>O<sub>2</sub> Assay Kit from Promega Corp. (Madison, WI). Cells were plated (60,000 cells/well) and the following day treated with CuO NPs (0.1 – 100 µg/mL; 0.08 – 80 µg Cu/mL) or CuSO<sub>4</sub> (80 µg Cu/mL) for 4 h. An aliquot of the media from each well was mixed with a derivatized luciferin substrate, which reacts directly with H<sub>2</sub>O<sub>2</sub> forming a luciferin precursor. The precursor is converted to luciferin and is detected in a coupled reaction with a recombinant luciferase enzyme, generating a luminescent signal that is proportional to H<sub>2</sub>O<sub>2</sub> concentration. tert-Butyl hydroperoxide (55 µM) in media was added to one column of wells without cells as a positive control of peroxide. The SpectraMax i3 plate reader with a luminescence cartridge was used to measure the luminescent signal.

### Detection of glutathione

IEC-6 cells were plated (60,000 cells/well) and the following day treated with CuO NPs (0.1 – 100 µg/mL; 0.08 – 80 µg Cu/mL) or CuSO<sub>4</sub> (80 µg Cu/mL) for 4 h. Glutathione (GSH) concentration in the cells was measured using the GSH-Glo™ Glutathione Assay kit from Promega Corp. (Madison, WI). In this assay, the cells are lysed and a derivatized luciferin substrate is added to the lysate. The luciferin substrate is converted to luciferin in the presence of GSH. GSH-S-transferase, which is supplied in the assay kit, catalyzes the reaction. Luciferin is detected in a coupled reaction with a recombinant luciferase enzyme, generating a luminescent signal that is proportional to GSH concentration. Glutathione (2.5 µM) in media was added to one column of wells without cells as a positive control. The SpectraMax i3 plate reader with a luminescence cartridge was used to measure the luminescent signal.

### Measurement of mitochondrial membrane potential

Mitochondrial membrane potential in IEC-6 cells was assessed with fluorescent microscopy using MitoTracker® Red CMXRos Red (Molecular Probes, Eugene, Oregon). Hoechst™ 33342 (Molecular Probes) was used to stain the nuclei. IEC-6 cells were plated to 30,000 cells per well in 96-well plates and left overnight in an incubator at 37 °C, 5% CO<sub>2</sub> and 95% relative humidity. The following day, the cells were treated with CuO NPs (0.1 – 100 µg/mL; 0.08 – 80 µg Cu/mL) or CuSO<sub>4</sub> (0.08 – 80 µg Cu/mL) for 4 h. One hour prior to staining, 80 µM carbonyl cyanide 4-(trifluoromethoxy)phenylhydrazone (FCCP) and 80 µM rotenone from Abcam (Cambridge, MA) in DMEM were added to non-treated cells in separate columns of the plate to serve as positive controls. Following exposure, cells were rinsed 2×

with PBS (37°C). Cells were stained with 10 µg/mL Hoechst 33342 and 200 nM Mitotracker in DMEM and delivered at 50 µl/well. The plate was returned to the incubator for 20 min. Cells were rinsed twice with DMEM followed by the addition of 4% paraformaldehyde (PFA, Sigma Aldrich) at 4 °C for 10 min as a fixative. The PFA-fixed cells were rinsed twice with DMEM to remove excess PFA and the plate was sealed with plate film.

Images of 2 fluorescent channels were sequentially captured and analyzed with a Thermo-Fisher Scientific (Waltham, MA) Array Scan XTI imaging platform, using a Zeiss 20× NeoFluar objective, a 7-color LED light source, and a Photometrics X1 CCD camera. Hoechst 33342 labeled cell images were captured using 386 nm excitation and 420–460 nm emission filter. Mitotracker labeled cell images were captured using a 560 nm excitation filter and a 584–645 nm emission filter.

Hoechst labeling was used to identify the nucleus; this signal was used to focus the image, define cellular nuclei and create objects via nuclear masks for measurement. The nuclear mask created by the instrument was used with the Organelle Health algorithm to measure area and fluorescence intensity of stained extranuclear mitochondria. The algorithm was programmed to measure at least 2000 selected objects per well, or measure objects from 20 fields, whichever came first.

## Data analysis

Data are displayed as mean ± standard deviation (SD) unless otherwise specified. The unit of measure was based on the number of wells tested. Cell viability data was analyzed by a two-way ANOVA with factors time and dose using Prism v6.07 (GraphPad, San Diego, CA). The level of significance was  $p < 0.05$ . If the ANOVA was significant, a Dunnett's multiple comparison test was done to compare untreated (control) cells to treated cells. Other data was analyzed using a one-way ANOVA with dose as the factor.

## Results

### Transmission Electron Microscopy

The CuO NPs were approximately spherical in shape and showed a primary size ranging from 20–50 nm (Supplementary Fig. 1). Particle aggregates incubated in cell assay media were in the range of 100–200 nm. The Cu<sub>2</sub>O-PVP NPs appeared to have a uniform shape and size (Supplementary Fig. 2). The shape was primarily cubic and there was a narrow size distribution of the NPs ( $48 \pm 7$ nm).

### Viability of rat IEC-6 cells

The results of CuO NPs on the viability of IEC-6 cells following a 4- or 24-h exposure are displayed in Figure 1. The two-way ANOVA indicated significant time ( $p < 0.0001$ ), dose ( $p < 0.0001$ ) and time\*dose interaction ( $p = 0.0002$ ) effects occurred. Cell viability was significantly decreased at CuO NPs concentrations 4 µg Cu/mL at each time point, with a greater response following 24 h exposure (75% cell viability at 4 h, 57% at 24 h). The highest dose, 80 µg Cu/mL, had the greatest effect on viability with approximately 25 and 12% of the cells viable at 4 and 24 h, respectively.

IEC-6 cells were incubated with Cu<sub>2</sub>O-PVP NPs at a dose range of 0.1 to 100 µg/mL (0.09 – 89 µg Cu/mL) for 24 h and the viability of the cells was measured (Fig. 2). Cell viability was significantly decreased ( $p < 0.0001$ ) at 44 and 89 µg/mL, with about a 35 and 75% decrease, respectively.

The cytotoxicity of CuO and Cu<sub>2</sub>O-PVP NPs was illustrated in the micrographs taken following 24 h exposure (Supplementary Fig. 3–7). The morphology of the cells treated with Cu<sub>2</sub>O-PVP NPs appeared normal at 22 µg Cu/mL in contrast to the cells treated with CuO NPs at 20 µg Cu/mL, which have begun to round up (Supplementary Fig. 4 and 5, respectively). At 80 µg Cu/mL CuO and 89 µg Cu/mL Cu<sub>2</sub>O, the change in cellular morphology was apparent with both NPs, but appeared to be greater with the CuO NPs, as some cells have broken apart with release of cellular contents (Supplementary Fig. 6 and 7, respectively).

The effect of Cu<sup>2+</sup> ions (from CuSO<sub>4</sub>) with respect to dose on IEC-6 cell viability following a 4- or 24-h exposure is shown in Fig. 3. Significant time, dose and time\*dose interaction effects ( $p < 0.0001$ ) were observed. A 4-h exposure to Cu<sup>2+</sup> ions resulted in significant increases in viability (about 10%) from 0.08 to 8 µg Cu/mL (Fig. 3). Cell viability was significantly decreased ( $p < 0.0001$ ) at 24 h with Cu<sup>2+</sup> ions at 40 and 80 µg Cu/mL.

The effect of Cu<sup>1+</sup> ions (from CuCl) with respect to dose on IEC-6 cell viability following a 4- or 24-h exposure is shown in Fig. 4. Significant time and dose effects ( $p < 0.0001$ ) were observed. A 4- and 24-h exposure to Cu<sup>1+</sup> ions resulted in a significant decrease in cell viability ( $p < 0.0001$ ) at 80 µg Cu/mL.

### Viability of human intestinal cells

CuO NPs were incubated with the 3-dimensional human intestinal model for 4 or 24 h to assess viability (Fig.1). The two-way ANOVA indicated significant time, dose and time\*dose interaction effects ( $p < 0.0001$ ) occurred. There was no effect of the CuO NPs up to 80 µg Cu/mL on viability of this model following a 4-h exposure. However, at 24 h, viability significantly decreased ( $p < 0.0001$ ) at 40 µg Cu/mL and 80 µg Cu/mL, with about a 20 and 60% decrease, respectively.

The dose effect of Cu<sub>2</sub>O-PVP NPs on viability of the human intestinal model was examined after a 24-h exposure (Fig. 2). Viability was significantly decreased ( $p < 0.0001$ ) at 44 µg Cu/mL and 89 µg Cu/mL, with about a 30 and 75% decrease, respectively.

The human intestinal model was exposed to CuSO<sub>4</sub> for 4 or 24 h (Fig. 3) at a dose range of 1 to 100 µg/mL (0.08 – 80 µg Cu/mL) and viability was assessed. The two-way ANOVA indicated significant time, dose and time\*dose interaction effects ( $p < 0.0001$ ) occurred. For the 4-h exposure, a slight (7%) but statistically significant increase ( $p < 0.05$ ) in viability was observed at 40 µg Cu/mL. No other effects were observed at 4 h. For the 24-h exposure, viability of the tissue was significantly decreased ( $p < 0.0001$ ) at 40 and 80 µg Cu/mL. The decrease in viability was 30 and 75%, respectively.

### Physico-chemical properties

The hydrodynamic diameter and zeta potential of NPs provide information on their size and dispersion, respectively. These parameters of the CuO and Cu<sub>2</sub>O-PVP NPs were measured in media following sonication and at the end of the exposure period (4 or 24 h) (Table 1). For CuO NPs, the hydrodynamic diameter increased with concentration following sonication and at 4 and 24 h after sonication, suggesting the particles were agglomerating. As concentration of the CuO NPs increased from 0.8 – 80 µg Cu/mL, the hydrodynamic diameter increased about 3.5-fold at all time points. The zeta potential of the CuO NPs following sonication and at 4 and 24 h post-sonication was below –15 mV. For the Cu<sub>2</sub>O-PVP NPs, the hydrodynamic diameter increased 1.4-fold following sonication and 1.12-fold at 24 h as concentration increased. The zeta potential remained below –15 mV. Overall, for both nanoparticles, the hydrodynamic diameter and zeta potential were similar over time. The dose-related increase in hydrodynamic diameter of the CuO NPs was dramatically lessened for the Cu<sub>2</sub>O-PVP NPs because of the PVP capping modification, which limits particle aggregation.

The polydispersity index (PDI) ranged from 0.447–0.604 for CuO NPs after sonication. Four and twenty-four h post-dosing (and sonication), the PDIs ranged from 0.591–0.73 and 0.563 – 1, respectively, for CuO NPs. For Cu<sub>2</sub>O-PVP NPs, the PDI after sonication ranged from 0.487–0.686 and at 24 h, from 0.608–0.686 (Table 1).

### Dissolution of CuO and Cu<sub>2</sub>O-PVP NPs

The dissolution of CuO and Cu<sub>2</sub>O-PVP NPs in media was examined over 24 h (Fig. 5). CuO NPs remained essentially as nanoparticles, with minimal dissolution to soluble Cu. Approximately 5% of the copper from CuO NPs became soluble over 24 h. In contrast, Cu<sub>2</sub>O-PVP NPs dissolved rapidly, with 80% of the total Cu detected in the filtrate within 1 h after the start of the incubation. The level of Cu<sub>2</sub>O-PVP NP dissolution then remained constant over the remaining course of the incubation period.

### Simulated gastrointestinal fluid treatment of CuO NPs

CuO NPs treated with pepsin at pH 2–6 showed pH dependence with respect to hydrodynamic diameter and zeta potential (Table 2). The NPs appeared to aggregate at pH 2 and 3. As pH increased within the pepsin-treated group, the hydrodynamic diameter of the particles decreased and the zeta potential became more negative, suggesting the particles became more disperse. Following incubation with pancreatin at pH 7, the hydrodynamic diameter ranged from 1132 to 1378 nm and the zeta potential from –19 to –28 mV. These parameters appeared to be stable. Following bile salt incubation, the hydrodynamic diameter ranged from 1001 to 1268 nm and the zeta potential ranged from –19 to –29 mV. Incubation with pancreatin and bile salts at pH 7 suggest minimal alteration of the particles with respect to hydrodynamic diameter and zeta potential.

The cytotoxicity of the simulated gastrointestinal fluid-treated CuO NPs was assessed in the IEC-6 cells for 4 or 24 h. The two-way ANOVA showed significant time, dose and time\*dose interaction effects ( $p < 0.0001$ ). At 4 h, a low but significant dose-related decrease in viability was detected at 0.08 µg Cu/mL. Viability decreased as dose increased to

about 30% viability at 80  $\mu\text{g Cu/mL}$  (Fig. 5). At 24 h (Fig. 6), significant decreases in viability were observed at 4  $\mu\text{g Cu/mL}$  and greater to about 30% viability.

### Detection of reactive oxygen species

The formation of reactive oxygen species by CuO NPs was assessed by measuring  $\text{H}_2\text{O}_2$  formation in IEC-6 cells 4 h after the addition of the NPs (Fig. 7). A significant increase in  $\text{H}_2\text{O}_2$  concentration was detected at 20  $\mu\text{g Cu/mL}$  ( $p < 0.01$ ). The CuO NP dose-related increase in  $\text{H}_2\text{O}_2$  was less than the positive control, tert-butyl hydroperoxide (55  $\mu\text{M}$ ) and  $\text{CuSO}_4$  (80  $\mu\text{g Cu/mL}$ ). The anti-oxidant GSH was measured in IEC-6 cell lysates 4 h post-exposure to CuO NPs. A dose-related decrease in GSH was detected at 0.08  $\mu\text{g Cu/mL}$  CuO NPs ( $p < 0.0001$ ) (Fig. 7).

### Depolarization of mitochondrial membrane potential

Mitochondria are organelles that can be affected by reactive oxygen species, with one effect displayed as increased mitochondrial membrane depolarization. A significant dose-related decrease in fluorescent mitochondrial marker intensity was observed at 0.08  $\mu\text{g Cu/mL}$  ( $p < 0.05$ ) after a 4-h incubation of IEC-6 cells with CuO NPs (Fig. 8). A significant decrease in fluorescent intensity was observed with  $\text{Cu}^{2+}$  ions, but the decrease was not observed until the concentration was 40  $\mu\text{g Cu/mL}$ .

## Discussion

Oral exposure to copper oxide NPs may occur by hand-to-mouth activity, ingestion of contaminated food or water, and secondary ingestion of inhaled particles. The toxicity of copper oxide NPs to the intestine is not well characterized. Ude et al. (2017) have recently reported on the dose-dependent decrease in viability of undifferentiated CaCo-2 intestinal epithelial cells by CuO NPs (size of 10 nm) and  $\text{CuSO}_4$ . Using *in vitro* rat two-dimensional and human three-dimensional intestinal models, we observed dose- and time-dependent cytotoxicity of two copper oxide NPs with approximate sizes (~50 nm), but different oxidation states. Another difference between the NPs was that a capping agent, PVP, was used to modify the surface of the  $\text{Cu}_2\text{O}$  NPs. PVP can limit the aggregation of NPs, which may in turn modify reactivity and dissolution of NPs (Hotze et al., 2010). Cytotoxicity evaluations  $\text{Cu}^{+1}$  and  $\text{Cu}^{2+}$  ions from  $\text{CuCl}$  and  $\text{CuSO}_4$ , respectively were also conducted. Dose- and time-dependent effects were observed for  $\text{Cu}^{2+}$  ions. The evaluation for  $\text{Cu}^{+1}$  ions was done only at 24 h, and dose-dependent effects were observed. The CuO NPs (oxidation state II) were more cytotoxic than the  $\text{Cu}_2\text{O}$ -PVP NPs (oxidation state I) and  $\text{Cu}^{2+}$  and  $\text{Cu}^{+1}$  ions in the rat cells at 24 h. Based on elemental Cu, the estimated lethal concentration<sub>50</sub> ( $\text{LC}_{50}$ ) at 24 h for the four copper agents in the IEC-6 cells were 8, 58, 58 and 65  $\mu\text{g Cu/mL}$ , respectively (Fig. 9, Table 3). The micrographs of IEC-6 cells exposed to CuO and  $\text{Cu}_2\text{O}$ -PVP NPs were consistent with potency of the NPs. The human *in vitro* intestinal model was less susceptible to cytotoxicity than the rat cells to the CuO NPs, with no effect observed at 4 h at a dose up to 80  $\mu\text{g Cu/mL}$  compared to a  $\text{LC}_{50}$  of 6  $\mu\text{g Cu/mL}$  for the rat cells. At 24 h, the  $\text{LC}_{50}$  of CuO NPs was 8 and 75  $\mu\text{g Cu/mL}$  for the rat and human models, respectively. For the  $\text{Cu}_2\text{O}$ -PVP NPs, the  $\text{LC}_{50}$  (58  $\mu\text{g Cu/mL}$ ) was about 7-fold higher than the value for CuO NPs with the human model at 24 h. Both model systems had similar responses to  $\text{Cu}^{2+}$

ions regarding viability, with no effect at 4 h at a dose range of 0.08 – 80  $\mu\text{g Cu/mL}$  and an  $\text{LC}_{50}$  of 58  $\mu\text{g Cu/mL}$  at 24 h.

Dissolution of NPs is a complex process related to its important role in the uptake, mechanism of toxicity and final disposition of the NP (Misra et al., 2012). Several components, such as size, surface area, and surface chemistry of the NPs and external factors such as exposure media and storage conditions can affect NP dissolution (Misra et al., 2012). Our dissolution study indicates that the  $\text{Cu}_2\text{O-PVP}$  NPs form Cu ions within 1 h after introduction into DMEM. In contrast, the dissolution of CuO NPs to Cu ions appears to be minimal over a 24 h incubation in DMEM. Líbalová et al. (2018) reported on the dissolution of CuO NPs (size, 12 nm) in water and DMEM. The CuO NPs were uncoated or coated with several capping agents including PVP. In water, there was minimal dissolution of the NPs. In DMEM, dissolution of the uncoated and PVP-coated CuO NPs to  $\text{Cu}^{2+}$  was about 55% at 1 h and 67% at 24 h. A study by Roesems et al. (2000) showed the importance of dissolution in the cytotoxicity of cobalt and cobalt tungsten particles (size 1–2  $\mu\text{m}$ ) to rat lung cells. Similar to the  $\text{Cu}_2\text{O-PVP}$  NPs, dissolution of these cobalt particles to ions appeared to have some role in the toxicity.

One proposed mechanism of NP toxicity is the generation of reactive oxygen species (ROS) (Abdal Dayem et al., 2017). ROS include oxygenated species such as  $\text{H}_2\text{O}_2$ , lipid peroxides, superoxide anion, and hydroxyl and peroxy radicals. Each of these species have different half-lives, with  $\text{H}_2\text{O}_2$  having the longest. In the rat cells, a dose-dependent increase in  $\text{H}_2\text{O}_2$  was detected following exposure to CuO NPs. Thiols such as GSH are part of the cellular anti-oxidant defense system. We observed a dose-dependent decrease in cellular GSH following exposure to CuO NPs. Several studies have shown the generation of oxidative stress by exposure to CuO NPs of various sizes in A549 cells (Karlsson et al., 2008), algae (Zhao et al., 2016), Caco-2 cells (Piret et al., 2012), human laryngeal epithelial (Hep-2) cells (Fahmy and Cormier, 2009), and human alveolar TT-1 cells (Misra et al., 2014). The mechanism of the formation of oxidants by copper is still under investigation. While redox cycling of Cu(I) and Cu(II) species, a Fenton-link reaction, is one proposed mechanism, Pham et al. (2013) have proposed the additional involvement of a Cu(III) species, which may significantly contribute to the redox cycling.

The mitochondrial membrane of the IEC-6 was affected by CuO NPs and  $\text{Cu}^{2+}$  ions, but the effect occurred at a lower dose of CuO NPs. Wang et al. (2012a) and Zhao et al. (2016) have reported mitochondrial membrane depolarization by CuO NPs in A549 cells and the algae *Chlorella pyrenoidosa*, respectively. NP-related formation of ROS appears to involve mitochondrial activity (Abdal Dayem et al., 2017). NPs depolarize the mitochondrial membrane and interfere with the electron-transport chain. This interference may involve NADPH-related enzymes and block the mitochondrial electron-transport chain. This results in increased superoxide anion levels by the transfer of electrons from the transport-chain carriers to oxygen. We observed CuO NP dose-related increases in  $\text{H}_2\text{O}_2$ , which is formed by disproportionation of superoxide anion and hydrogen ion, catalyzed by superoxide dismutase. Also observed was mitochondrial membrane depolarization by CuO NPs at concentrations less than observed with the  $\text{Cu}^{2+}$  ions.

There may be other mechanisms of CuO NP induced cytotoxicity in addition to formation of ROS. IEC-6 cells treated with CuSO<sub>4</sub> at 80 µg Cu/mL had the highest level of H<sub>2</sub>O<sub>2</sub> and levels of GSH approximately 50% of control at 4 h. However, at this time and dose, viability of the cells was not affected by CuSO<sub>4</sub>. In contrast, CuO NPs significantly decreased IEC-6 cell viability by about 25% at a dose of 4 µg Cu/mL by 4 h post-exposure. Also, the IEC-6 mitochondrial membrane was significantly depolarized by CuO NPs at doses lower than observed with CuSO<sub>4</sub> 4 h post-exposure. The reason for this disparity in effect between CuO NPs and Cu<sup>2+</sup> is not known.

The dissolution results suggest that the Cu ions have a role in the cytotoxicity of Cu<sub>2</sub>O-PVP NPs in the rat and human intestinal models. The LC<sub>50</sub> of Cu<sub>2</sub>O-PVP NPs at 24 h in IEC-6 cells and human intestinal model were the same as observed with Cu<sup>2+</sup> (58 µg Cu/mL). For CuO NPs, it appears that these particles have inherent cytotoxic properties, as their dissolution was minimal. Thus, for toxicity to occur, the NPs would need to be taken up by the cells. Wang et al. (2012a), using TEM, reported that CuO NPs were present internally in A549 cells and the mechanism of uptake was most likely endocytosis. Studies in A549 cells suggest that CuO NPs have inherent toxicological properties (Karlsson et al., 2008; Midlander et al., 2009). These toxicological properties of the CuO NPs are dependent on the physical and chemical properties of the CuO NP used and the experimental conditions. CuO NPs can vary in size, surface coatings and reactivity and other factors. Misra et al. (2014) examined the cytotoxicity of CuO NPs in different shapes (rods, spheres and spindles) and found that biological response was due to the particulate form upon immediate exposure to the cells, but at later times (24 h and greater) the dissolved ions contributed more to the cytotoxic effect.

While pristine NPs are used in many *in vitro* toxicity studies, in the real world, NPs may be altered chemically or physically before an organism is exposed or the NPs reach a target organ. This alteration could entail weathering of the NP by the external environment (e.g., sunlight) or modification by a biological process. For oral exposures, NPs would encounter gastrointestinal fluids which may modify the particle, which in turn could alter uptake or a potential toxic effect in the gastrointestinal system. Thus, it is important to consider the state of the NP with respect to real world exposures. There are some studies on potential cytotoxic alteration of NPs by GI fluids. McCracken et al. (2013) observed no cytotoxic effect of pristine SiO<sub>2</sub> and TiO<sub>2</sub> NPs or those pre-treated with GI fluids in human intestinal C2BBel1 cells (a Caco-2 clone). Böhmert et al. (2014) reported minimal differences in the cytotoxicity of pristine Ag NPs or pre-treated with GI fluids in Caco-2 cells. In our study with CuO NPs pre-treated with simulated GI fluids and exposed to rat IEC-6 cells, we observed some slight enhancement of cytotoxicity at the low dose range. The major GI fluid effect on the CuO NPs was physico-chemical, regarding zeta potential and hydrodynamic diameter. Ingested NPs will contact GI fluids at varying pHs. The pH of the stomach fluid in the fasted state is approximately 2. At the lowest pH (2) in our study, the hydrodynamic diameter was the highest (and zeta potential the least negative), suggesting the CuO NPs were binding to each other, to pepsin or both to form a large agglomerate. The binding to pepsin would form a protein corona. Böhmert et al. (2014) observed similar changes in hydrodynamic diameter (reported as radius) of Ag NPs at low pH. In the presence of food, the stomach pH can vary from 4–7 (Marques et al., 2011). A pH dependent change in

hydrodynamic diameter and zeta potential of the CuO NPs was observed when the pH was increased from 2 to 6 for the simulated stomach fluid, suggesting less agglomeration of the particles. The hydrodynamic diameter and zeta potential appeared to have become steadied with incubation of pancreatin and bile salts at pH 7. The diameter was less than observed for the stomach fluid at pH 2 and the zeta potential was more negative. Böhmert et al. (2014) reported similar results with Ag NPs when the fluid was changed from stomach to intestinal, with an increase of pH.

The development of cellular models has advanced today such that *in vitro* three-dimensional models can be readily grown, having greater complexity than two-dimensional models (Antoni et al., 2015; Edmondson et al., 2014). The three-dimensional model we used consists of human enterocytes, Paneth cells, M cells and intestinal stem cells. The two-dimensional model consists of rat intestinal enterocytes. The microenvironment of cells in a three-dimensional model is different than in a two-dimensional model. With the former model, the different cell types interact with each other regarding spatial arrangement in contrast to two-dimensional models, which grow as a monolayer. The cellular interaction in the three-dimensional model can impact cell proliferation, differentiation, morphology, expression of genes and proteins and responses of the cells to external stimuli (Edmondson et al., 2014). We observed that the cells of the three-dimensional model of the human intestine were less affected by exposure to CuO NPs than the cells of the two-dimensional model. No effect was observed following 4 h exposure to both the CuO NPs in the human three-dimensional model, and higher concentrations of CuO, Cu<sub>2</sub>O-PVP and Cu<sup>2+</sup> were required to elicit a cytotoxic effect by 24 h. With the two-dimensional model, all the cells in the monolayer are basically exposed to the test compounds, whereas, with the three-dimensional model, the test chemical initially contacts the upper layer of the tissue when first dosed and must either diffuse or be transported into the lower layers over time. Differences in the response may be due to the species of origin for each model (rat vs. human). The cells in the human three-dimensional model may be able to repair themselves more easily than the rat two-dimensional model.

## Conclusion

CuO and Cu<sub>2</sub>O-PVP NPs and Cu<sup>1+</sup> and Cu<sup>2+</sup> ions decreased the viability of rat IEC-6 cells (two-dimensional model) and human intestinal cells (three-dimensional model). The CuO NPs were more cytotoxic than the Cu<sub>2</sub>O-PVP NPs and Cu<sup>1+</sup> and Cu<sup>2+</sup> ions in the rat cells. The CuO NPs were also more cytotoxic to the rat two-dimensional intestinal model than the human three-dimensional model. We also observed that the CuO NPs were more stable in media over time than the Cu<sub>2</sub>O-PVP NPs, which may explain in part their higher cytotoxic potential. Reactive oxygen species are formed following incubation of CuO NPs with IEC-6 cells, which may be a mechanism of action of these NPs. Treatment of CuO NPs with simulated GI fluids had a slight effect on the cytotoxic potential of these NPs relative to pristine CuO NPs. Overall, it is important to consider the valence state of the NPs, test model system used (two- vs. three-dimensional) as well the physical and chemical condition of the NPs when assessing their cytotoxic potential.

## Supplementary Material

Refer to Web version on PubMed Central for supplementary material.

## Acknowledgements:

The authors thank Drs. David Thomas and William Boyes for their review of an earlier version of this manuscript.

This work was supported by internal funds from the Office of Research and Development, U.S. Environmental Protection Agency.

## References

- Abdal Dayem A, Hossain MK, Lee SB, Kim K, Saha SK, Yang G-M, Choi HY, Cho S-G, 2017 The role of reactive oxygen species (ROS) in the biological activities of metallic nanoparticles. *International Journal of Molecular Sciences* 18 (1), 120.
- Antoni D, Burckel H, Josset E, Noel G, 2015 Three-dimensional cell culture: a breakthrough in vivo. *International Journal of Molecular Sciences* 16 (3), 5517–5527. [PubMed: 25768338]
- Böhmert L, Girod M, Hansen U, Maul R, Knappe P Niemann B, et al., 2014 Analytically monitored digestion of silver nanoparticles and their toxicity on human intestinal cells. *Nanotoxicology* 8 (6), 631–642. [PubMed: 23763544]
- Chang YN, Zhang M, Xia L, Zhang J, Xing G, 2012 The toxic effects and mechanisms of CuO and ZnO nanoparticles. *Materials* 5 (12), 2850–2871.
- Di Bucchianico S, Fabbri MR, Misra SK, Valsami-Jones E, Berhanu D, Reip P, et al., 2013 Multiple cytotoxic and genotoxic effects induced by in vitro by differently shaped copper oxide nanomaterials. *Mutagenesis* 28 (3), 287–299. [PubMed: 23462852]
- Elder A, Vidyasagar S, DeLouise L, 2009 Physicochemical factors that affect metal and metal oxide nanoparticle passage across epithelial barriers. *Wiley Interdisciplinary Reviews in Nanomedicine and Nanobiotechnology* 1(4), 434–450. [PubMed: 20049809]
- Edmondson R, Broglie JJ, Adcock AF, Yang L, 2014 Three-dimensional cell culture systems and their applications in drug discovery and cell-based biosensors. *Assay and Drug Development Technologies* 12 (4), 207–218. [PubMed: 24831787]
- Fahmy B, Cormier SA, 2009 Copper oxide nanoparticles induce oxidative stress and cytotoxicity in airway epithelial cells. *Toxicology in Vitro* 23 (7), 1365–1371. [PubMed: 19699289]
- Fröhlich E, 2013 Cellular targets and mechanisms in the cytotoxic action of non-biodegradable engineered nanoparticles. *Current Drug Metabolism* 14 (9), 976–988. [PubMed: 24160294]
- Holder AL, Goth-Goldstein R, Lucas D, Koshland CP 2012 Particle-induced artifacts in the MTT and LDH assays. *Chemical Research in Toxicology* 25 (9), 1885–1892. [PubMed: 22799765]
- Hotze EM, Phenrat T, Lowry GV 2010 Nanoparticle aggregation: challenges to understanding transport and reactivity in the environment. *Journal of Environmental Quality* 39 (6), 1909–1924. [PubMed: 21284288]
- Karlsson HL, Cronholm P, Gustafsson J, Möller L, 2008 Copper oxide nanoparticles are highly toxic: a comparison between metal oxide nanoparticles and carbon nanotubes. *Chemical Research in Toxicology* 21 (9), 1726–1732. [PubMed: 18710264]
- Keller AA, Lazareva A, 2014 Predicted releases of engineered nanomaterials: from global to regional to local. *Environmental Science & Technology Letters* 1 (1), 65–70.
- Kermanizadeh A, Balharry D, Wallin H, Loft S, Møller P, 2015 Nanomaterial translocation – the biokinetics, tissue accumulation, toxicity and fate of materials in secondary organs – a review. *Critical Reviews in Toxicology* 45 (10), 837–872. [PubMed: 26140391]
- Landsiedel R, Fabian E, Ma-Hock L, Wohlleben W, Wiench K, Oesch F, et al., 2012 Toxicity/biokinetics of nanomaterials. *Archives of Toxicology* 86 (7), 1021–1060. [PubMed: 22576463]
- Lefebvre DE, Venema K, Gombau L, Valerio LG Jr., Raju J, Bondy GS, et al., 2015 Utility of models of the gastrointestinal tract for assessment of the digestion and absorption of engineered nanomaterials released from food matrices. *Nanotoxicology* 9(4), 523–542. [PubMed: 25119418]

- Líbalová H, Costa PM, Olsson M, Farcál L, Ortelli S, Blosi M, et al., 2018 Toxicity of surface-modified copper oxide nanoparticles in a mouse macrophage cell line: interplay of particles, surface coating and particle dissolution. *Chemosphere* 196, 482–493. [PubMed: 29324388]
- Marques MRC, Loebenberg R, Almukainzi M, 2011 Simulated biological fluids with possible application in dissolution testing. *Dissolution Technologies* 18 (3), 15–28.
- McCracken C, Zane A, Knight DA, Dutta PK, Waldman WJ, 2013 Minimal intestinal epithelial cell toxicity in response to short- and long-term food-relevant inorganic nanoparticle exposure. *Chemical Research in Toxicology* 26 (10), 1514–1525. [PubMed: 24028186]
- McSweeney PC, 2017 The safety of nanoparticles in sunscreens: an update for general practice. *Australian Family Physician* 45 (6), 397–399.
- Midlander K, Cronholm P, Karlsson HL, Elihn K, Möller L, Leygraf C, et al., 2009 Surface characteristics, copper release, and toxicity of nano- and micrometer-sized copper and copper(II) oxide particles: a cross-disciplinary study. *Small* 5 (3), 389–399. [PubMed: 19148889]
- Misra SK, Dybowska A, Berhanu D, Luoma SN, Valsami-Jones E, 2012 The complexity of nanoparticle dissolution and its importance in nanotoxicological studies. *Science of the Total Environment* 438, 225–232. [PubMed: 23000548]
- Misra SK, Nuseibeh S, Dybowska A, Berhanu D, Tetley TD, Valsami-Hones E, 2014 Comparative study using spheres, rods and spindle-shaped nanoplatelets on dispersion stability, dissolution and toxicity of CuO nanomaterials. *Nanotoxicology* 8 (4), 422–432. [PubMed: 23590525]
- Petersen EJ, Henry TB, Zhao J, MacCuspie RI, Kirschling TL, Dobrovolskaia MA, et al., 2014 Identification and avoidance of potential artifacts and misinterpretations in nanomaterial ecotoxicity measurements. *Environmental Science & Technology* 48 (8), 4226–4246. [PubMed: 24617739]
- Pham AN, Xing G, Miller CJ, Waite TD, 2013 Fenton-like copper redox chemistry revisited: hydrogen peroxide and superoxide mediation of copper-catalyzed oxidant production. *Journal of Catalysis* 301, 54–64.
- Piret JP, Vankoningsloo S, Mejia J, Noël F, Boilan E, Lambinon F, et al., 2012 Differential toxicity of copper (II) oxide nanoparticles of similar hydrodynamic diameter on human differentiated intestinal Caco-2 cell monolayers is correlated in part to copper release and shape. *Nanotoxicology* 6 (7), 789–803. [PubMed: 22023055]
- Roesms G, Hoet PHM, Dinsdale D, Demedts M, Nemery B, 2000 In vitro cytotoxicity of various forms of cobalt for rat alveolar macrophages and Type II pneumocytes. *Toxicology and Applied Pharmacology* 162 (1), 2–9. [PubMed: 10631122]
- Sanders K, Degn LL, Mundy WR, Zucker RM, Dreher K, Zhao B, et al. 2012 In vitro phototoxicity and hazard identification of nano-scale titanium dioxide. *Toxicology and Applied Pharmacology* 258 (2), 226–236. [PubMed: 22115978]
- Thit A, Selck H, Bjerregaard JF, 2015 Toxic mechanisms of copper oxide nanoparticles in epithelial kidney cells. *Toxicology in Vitro* 29 (5), 1053–1059. [PubMed: 25862124]
- Ude VC, Brown DM, Viale L, Kanase N, Stone V, Johnston HJ, 2017 Impact of copper oxide nanomaterials on differentiated and undifferentiated Caco-2 intestinal epithelial cells; assessment of cytotoxicity, barrier integrity, cytokine production and nanomaterial penetration. *Particle and Fibre Toxicology* 14, 31. [PubMed: 28835236]
- Vimbela GV, Ngo SM, Frazee C, Yang L, Stout DA, 2017 Antibacterial properties and toxicity from metallic nanomaterials. *International Journal of Nanomedicine* 12, 3941–3965. [PubMed: 28579779]
- Wang Z, Li N, Zhao J, White JC, Qu P, Xing B, 2012a CuO nanoparticle interaction with human epithelial cells: cellular uptake, location, export, and genotoxicity. *Chemical Research in Toxicology* 24 (7), 1512–1521.
- Wang Y, Zi X-Y, Su J, Zhang H-X, Zhang X-R, Zhu HY, et al., 2012b Cuprous oxide nanoparticles selectively induce apoptosis of tumor cells. *International Journal of Nanomedicine* 7, 2641–2652. [PubMed: 22679374]
- Yang Q, Wang Y, Yang Q, Gao Y, Duan X, Fu Q, et al., 2017 Cuprous oxide nanoparticles trigger ER stress-induced apoptosis by regulating copper trafficking and overcoming resistance to sunitinib therapy in renal cancer. *Biomaterials* 147, 72–85.

Zhao J, Cao X, Liu X, Wang Z, Zhang C, Whit JC, et al., 2016 Interactions of CuO nanoparticles with the algae *Chlorella pyrenoidosa*: adhesion, uptake, and toxicity. *Nanotoxicology* 10 (9), 1297–1305. [PubMed: 27345461]

EPA Author Manuscript

EPA Author Manuscript

EPA Author Manuscript

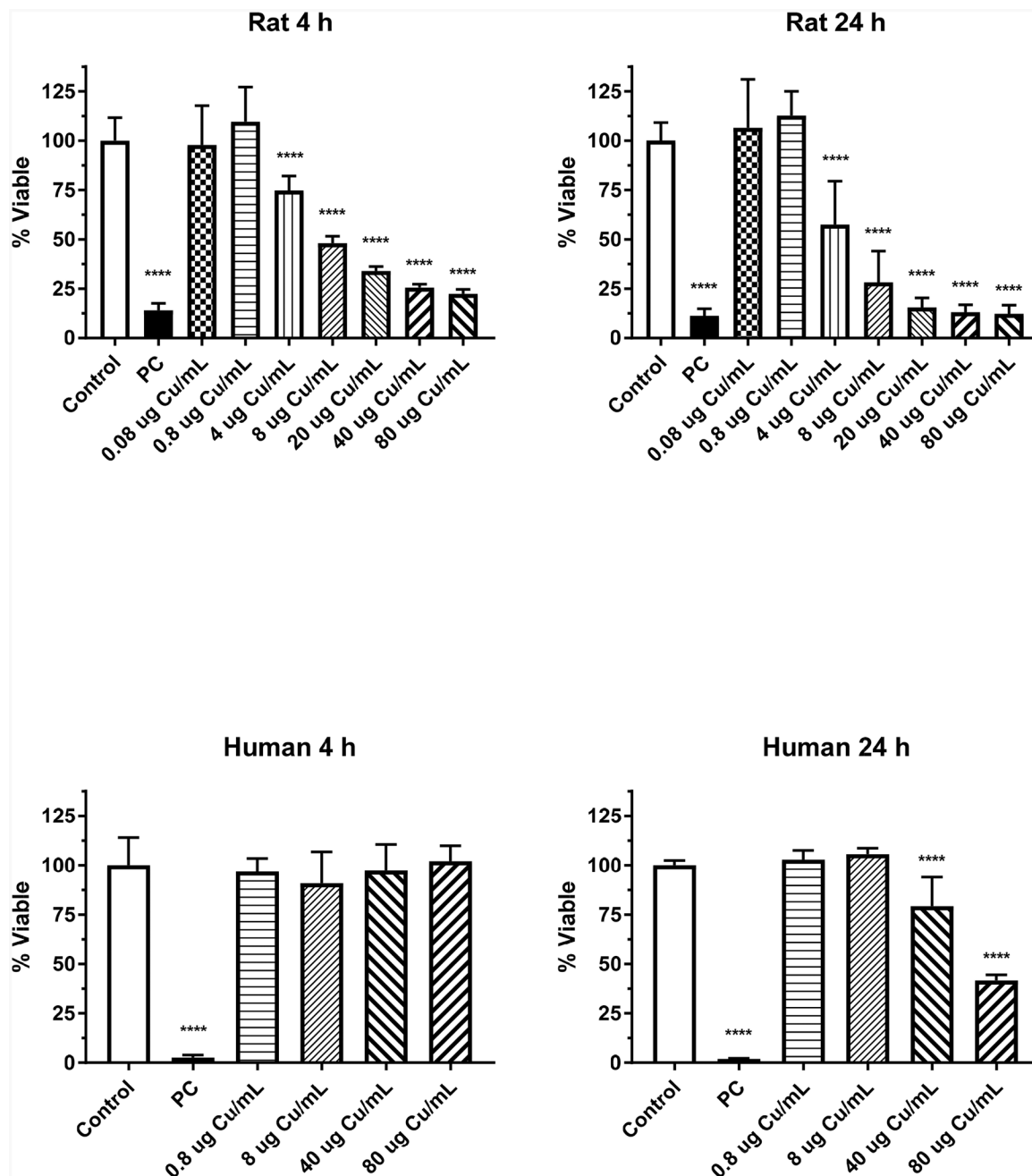


**Figure 1.** Cytotoxicity of CuO NPs in rat IEC-6 and human EpiIntestinal™ cells following 4- or 24-h exposure. Data based on  $\mu\text{g Cu/mL}$  and represents mean  $\pm$  SD, N= 10–11 for the rat cells and N=8 for the human cells. \*\*\*\*, significantly different from control,  $p < 0.0001$ . PC represents positive control, 0.3% Triton X-100 in distilled water.

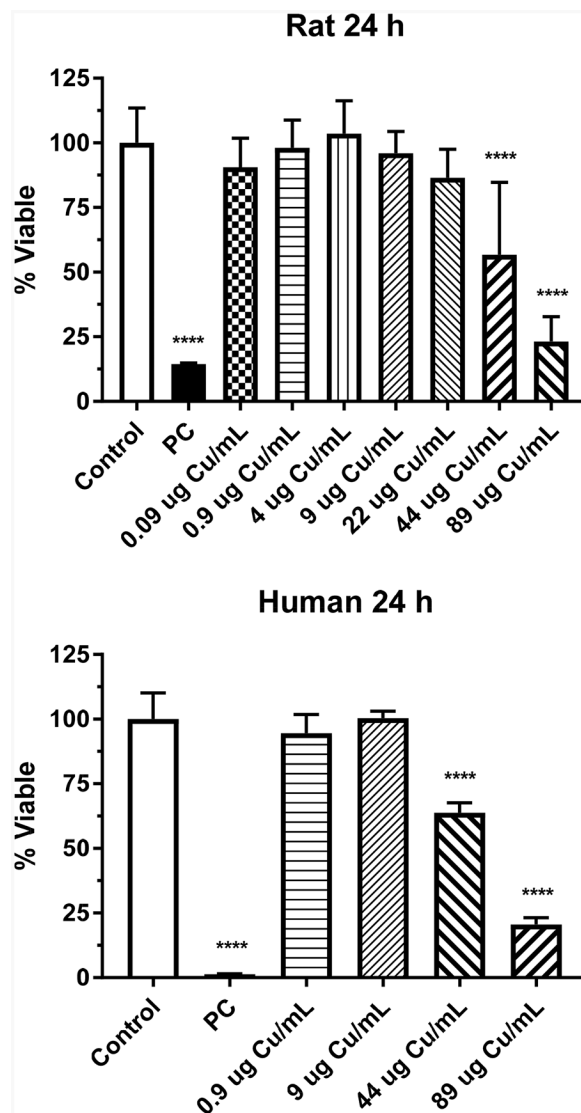


**Figure 2.** Cytotoxicity of Cu<sub>2</sub>O-PVP NPs in rat IEC-6 and human EpiIntestinal™ cells following 24-h exposure. Data based on  $\mu\text{g Cu/mL}$  and represents mean  $\pm$  SD, N= 11–12 for the rat cells and N=8 for the human cells. \*\*\*\*, significantly different from control,  $p < 0.0001$ . PC represents positive control, 0.3% Tritox X-100 in distilled water.

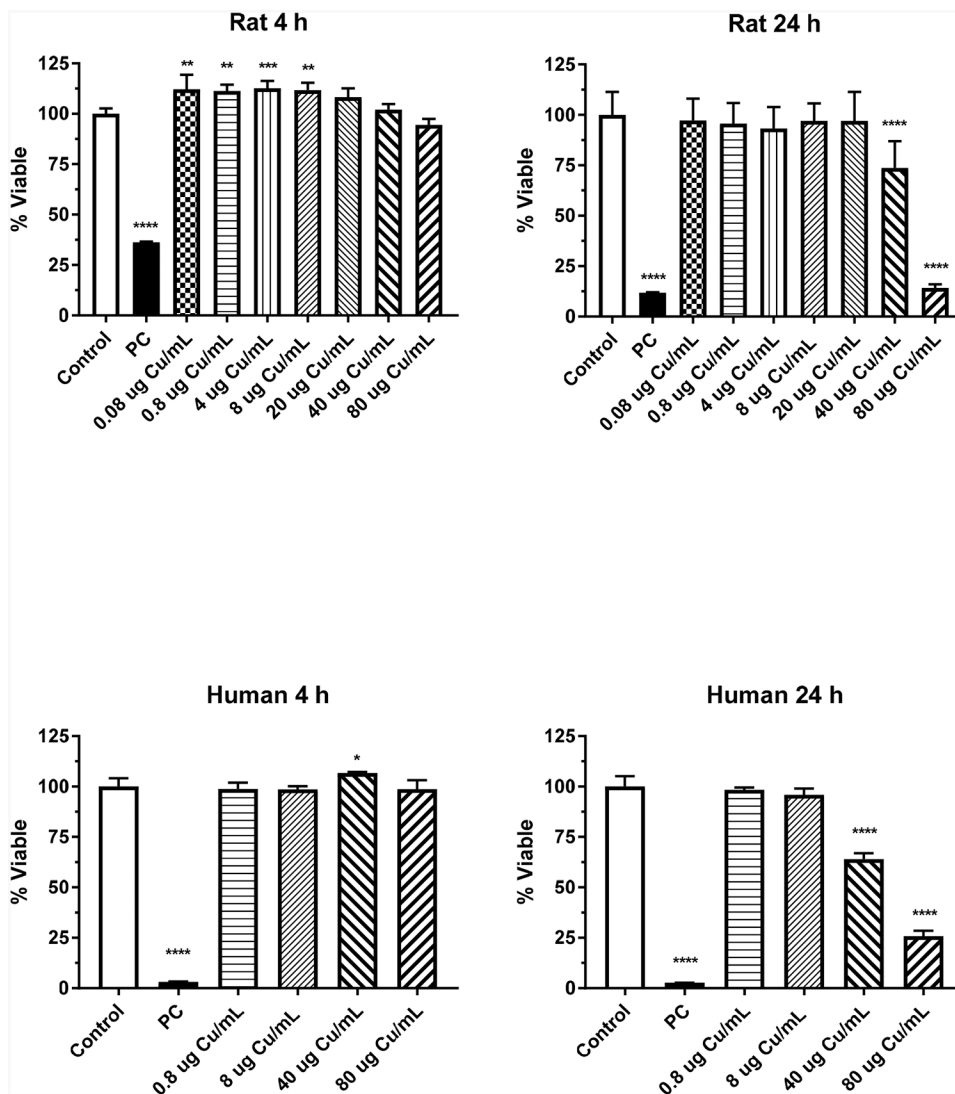


**Figure 3.** Cytotoxicity of CuSO<sub>4</sub> in rat IEC-6 and human EpiIntestinal™ cells following 4- or 24-h exposure. Data based on μg Cu/mL and represents mean ± SD, N= 11–12 for the rat cells and N=8 for the human cells. \*\*, significantly different from control, p < 0.01; \*\*\*, significantly different from control, p < 0.001; \*\*\*\*, significantly different from control, p < 0.0001. PC represents positive control, 0.3% Tritox X-100 in distilled water.

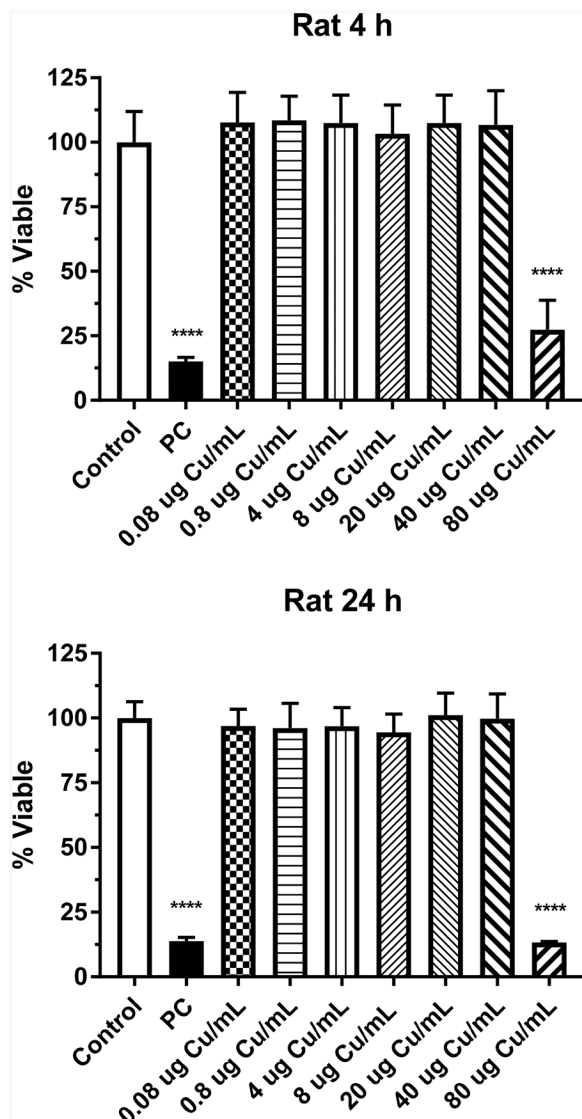


**Figure 4.** Cytotoxicity of CuCl in rat IEC-6 cells following 4- or 24-h exposure. Data based on  $\mu\text{g}$  Cu/mL and represents mean  $\pm$  SD, N= 11–12. \*\*\*\*, significantly different from control,  $p < 0.0001$ . PC represents positive control, 0.3% Tritox X-100 in distilled water.

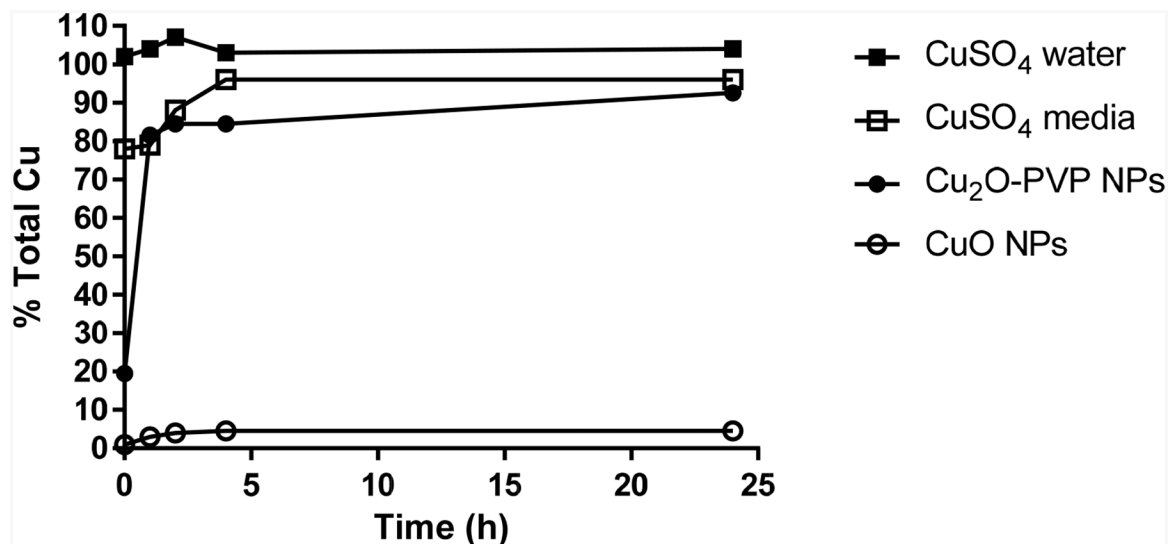


**Figure 5.** Percent total dissolved copper over time following incubation (37 °C) of CuO NPs (○), Cu<sub>2</sub>O-PVP NPs (●) and CuSO<sub>4</sub> in media (◻) or water (◼). Ten ppm Cu in the form of CuO, Cu<sub>2</sub>O-PVP and CuSO<sub>4</sub> was incubated in media or water and samples removed up to 24 h. Aqueous samples were filtered. The filtrate was hot plate digested in acid. The digest was diluted with water and analyzed by inductively coupled plasma optical emission spectrometry. Data represents % total copper in solution, N=2.

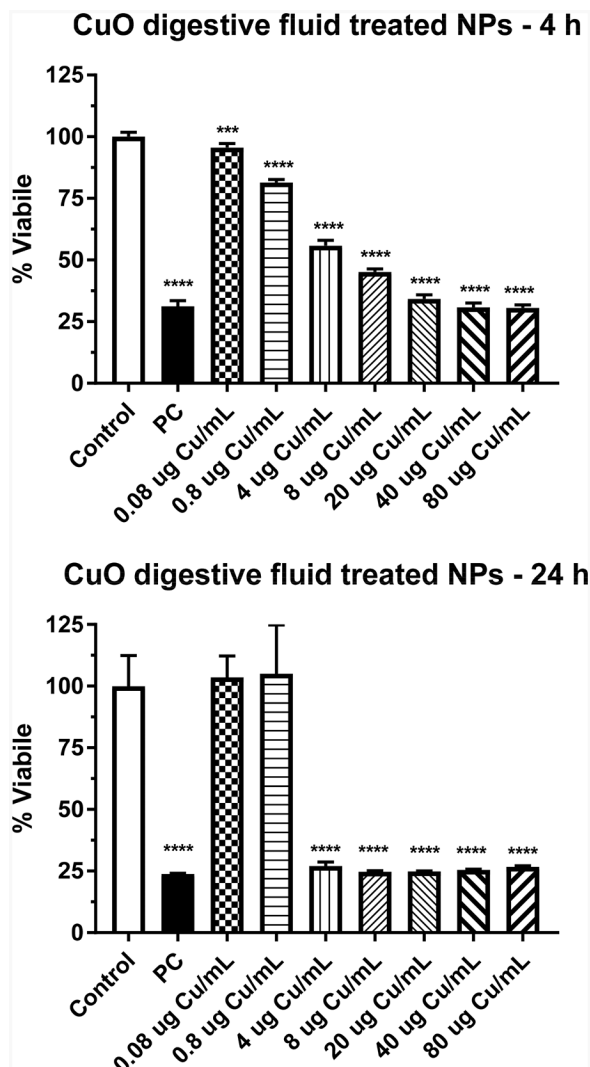


**Figure 6.**

CuO NPs were treated with simulated gastrointestinal fluids as described in the methods. After isolating the NPs following the last treatment, the NPs were resuspended in media and probe sonicated. IEC-6 cells were dosed with the treated NPs for 4 (A) or 24 (B) h and viability was assessed. Data represents mean  $\pm$  SD, N= 6. PC is positive control, 0.1% Tritox X-100. \*\*\*, significantly different from control,  $p < 0.001$ ; \*\*\*\*, significantly different from control,  $p < 0.0001$

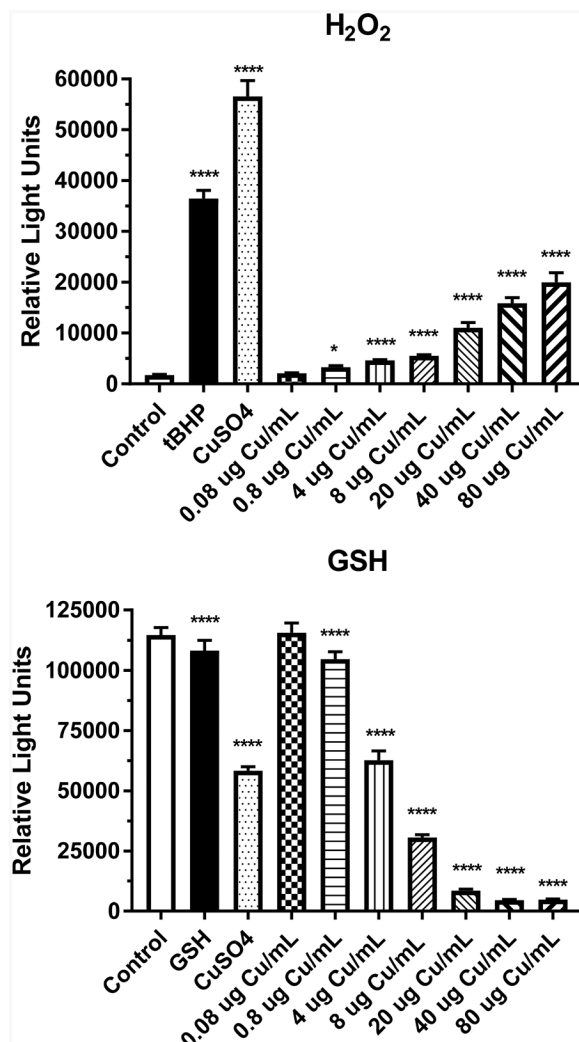


**Figure 7.** Luminescent detection of H<sub>2</sub>O<sub>2</sub> and GSH in rat IEC-6 cells following a 4-h exposure to media (control), CuSO<sub>4</sub> (80 µg Cu/mL), or CuO NPs (0.08 – 80 µg Cu/mL). t-Butyl hydroperoxide (tBHP, 55 µM) was used as a positive control in the H<sub>2</sub>O<sub>2</sub> experiment and 2.5 µM GSH in the GSH experiment. Data represents mean ± SD, N= 12 for the H<sub>2</sub>O<sub>2</sub> and GSH experiments. \*, significantly different from control, p < 0.05; \*\*\*\*, significantly different from control, p < 0.0001.

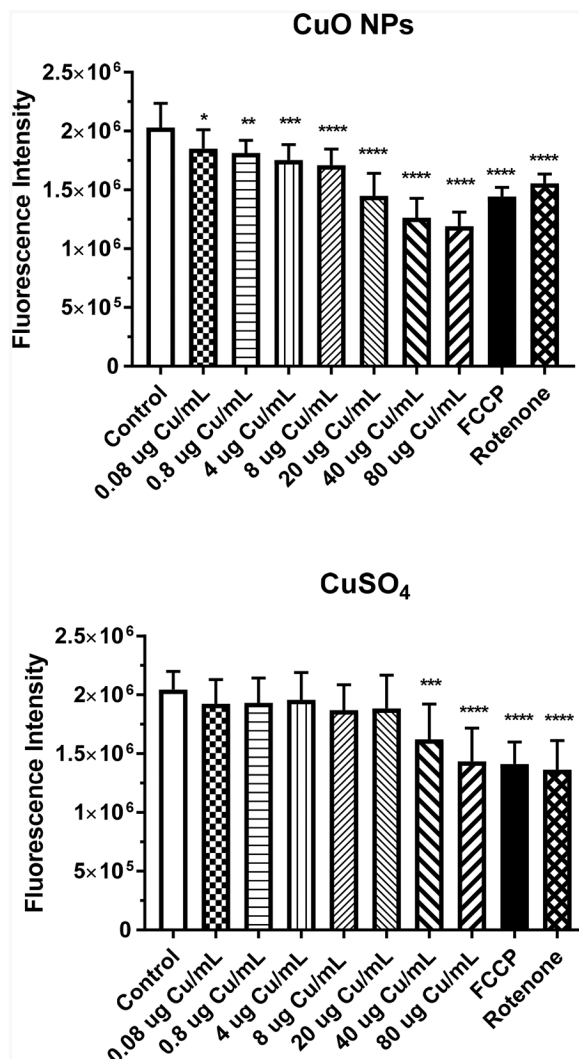


**Figure 8.**

Intensity of mitochondrial fluorescence following a 4-h incubation of IEC-6 cells with CuO NPs (A) or CuSO<sub>4</sub> (B). Control represents media alone. FCCP and rotenone (80 μM) were the positive controls. Data (μg Cu/mL) represents mean ± SD, n=12. \*, significantly different from control, p < 0.05; \*\*, significantly different from control, p < 0.01; \*\*\*, significantly different from control, p < 0.001; \*\*\*\*, significantly different from control, p < 0.0001.

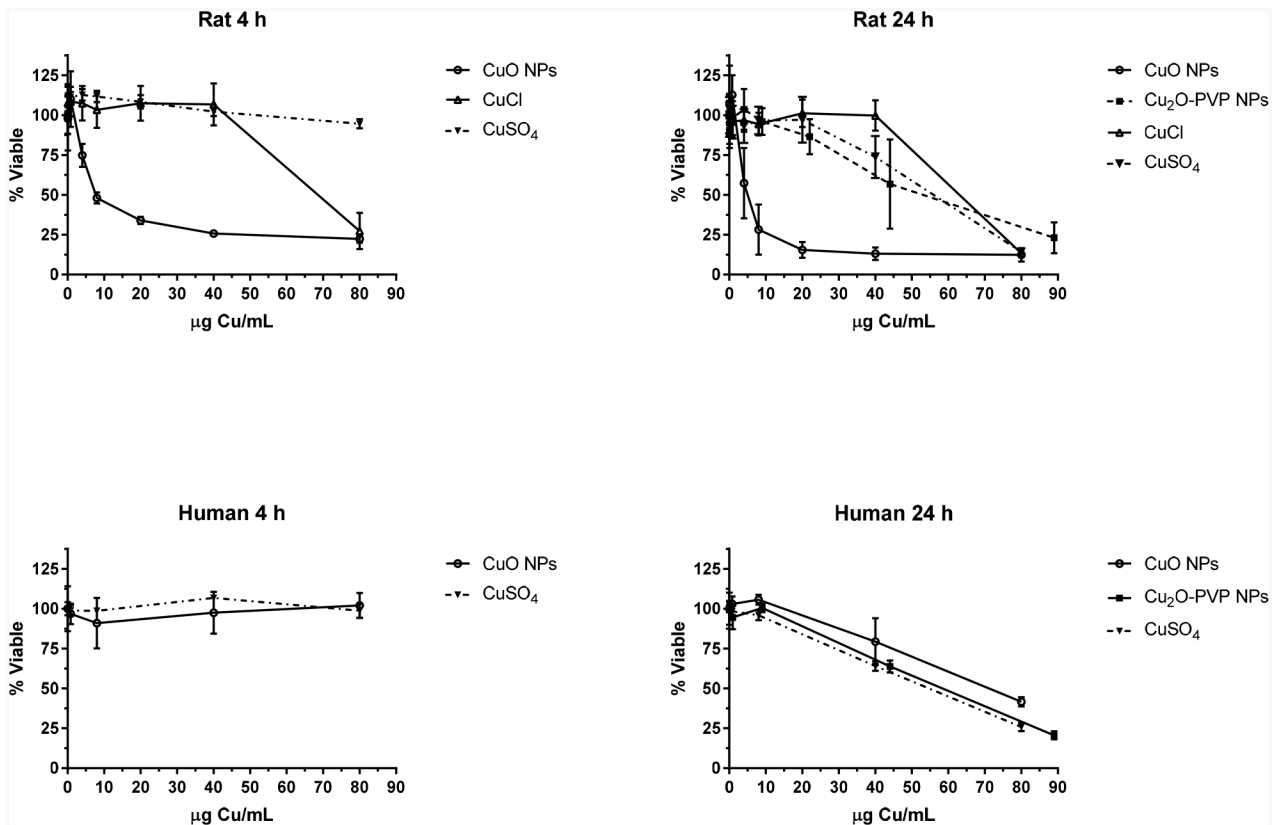


**Figure 9.** Cytotoxicity of CuO NPs, Cu<sub>2</sub>O-PVP NPs, CuCl and CuSO<sub>4</sub> in rat and human intestinal models at 4 and 24 h. Data is based on µg Cu/mL. Data represents mean ± SD, N = 4–12.

**Table 1**

Hydrodynamic diameter (HD), zeta potential (ZP) and polydispersity index (PDI) of CuO and Cu<sub>2</sub>O-PVP NPs in media after sonication and 4 or 24-h after sonication

Nanoparticle	Incubation Time (h)	Concentration ( $\mu\text{g Cu/mL}$ )	After sonication			4 or 24 h after sonication		
			HD (nm)	ZP (mV)	PDI	HD (nm)	ZP (mV)	PDI
CuO	4	0.8	381.2 <sup>b</sup>	-11.1	0.525	395.2	-11.1	0.591
		8	533.1	-12.2	0.515	526.7	-13.5	0.612
		40	817.3	-13.6	0.561	722.1	-11.9	0.730
		80	1347.1	-10.5	0.467	1338.0	-6.7	0.701
CuO	24	0.8	341.6	-10.6	0.447	310.6	-10.1	0.563
		8	548.3	-13.3	0.482	558.7	-13.4	0.782
		40	947.9	-13.2	0.604	826.5	-13.0	0.691
		80	1501.2	-13.5	0.464	1442.6	-12.5	1.000
Cu <sub>2</sub> O-PVP	24	0.9	389.3	-12.5	0.686	408.3	-12.4	0.608
		9	413.3	-11.6	0.606	365.5	-12.8	0.686
		44	436.1	-14.2	0.594	535.8	-12.6	0.634
		89	536.1	-12.7	0.487	456.4	-14.2	0.663

Media with 10% FBS was measured for hydrodynamic diameter, zeta potential and polydispersity index. The values were 45 nm, -7.8 mV and 0.252, respectively.

**Table 2**

Effect of simulated gastrointestinal fluids on hydrodynamic diameter, polydispersity index and zeta potential of CuO nanoparticles

Gastric fluid	Treatment group <sup>b</sup>	Hydrodynamic diameter (nm)	Polydispersity Index	Zeta potential <sup>c</sup> (mV)
Pepsin <sup>a</sup>	1	5104	0.264	-3.4 ± 0.5
	2	3527	0.320	-14.8 ± 1.0
	3	1607	0.258	-38.9 ± 0.8
	4	1631	0.287	-31.7 ± 1.7
	5	1534	0.282	-27.1 ± 1.3
Pancreatin	1	1378	0.318	-23.6 ± 1.3
	2	1238	0.253	-27.5 ± 0.8
	3	1215	0.233	-19.2 ± 0.8
	4	1260	0.219	-19.5 ± 0.8
	5	1232	0.276	-19.0 ± 0.4
Bile salts	1	1268	0.370	-26.4 ± 0.7
	2	1005	0.273	-29.0 ± 0.4
	3	1001	0.259	-20.3 ± 0.5
	4	1003	0.241	-21.9 ± 0.8
	5	1014	0.242	-18.9 ± 0.3

<sup>a</sup>Nanoparticles (1 mg/mL, 0.8 mg Cu/mL) were treated sequentially with pepsin, pancreatin and bile salts. Samples were ultracentrifuged following each treatment. The pellet was resuspended before measurement of zeta potential and hydrodynamic diameter.

<sup>b</sup>Nanoparticles were incubated with pepsin at either pH 2 (Group 1), pH 3 (Group 2), pH 4 (Group 3), pH 5 (Group 4) or pH 6 (Group 5). All incubations with pancreatin and bile salts were done at pH 7.

<sup>c</sup>mean ± SD, n=3.

**Table 3**

Concentration of CuO and Cu<sub>2</sub>O-PVP NPs and copper (I) chloride and copper(II) sulfate decreasing viability of rat IEC-6 and human intestinal cells by 50% (LC<sub>50</sub>).

Chemical	Species	Time (h)	LC <sub>50</sub> (µg Cu/mL) <sup>a</sup>
CuO	Rat	4	6
		24	8
	Human	4	No effect
		24	75
Cu <sub>2</sub> O-PVP	Rat	24	58
		Human	24
CuSO <sub>4</sub>	Rat	4	No effect
		24	58
		Human	4
		24	58
		Human	24
CuCl	Rat	4	70
		24	65

<sup>a</sup>Data from Figure 9.